mathematical biology, we have provided a unified picture of what happened on the Millennium Bridge five years ago, both for the bridge vibrations and the crowd dynamics. The approach suggested here may also prove useful for estimating the damping needed to safeguard other bridges, present and future, against synchronous lateral excitation by pedestrians.

Steven H. Strogatz*, Daniel M. Abrams*, Allan McRobie†, Bruno Eckhardt‡§, Edward Ott‡
*Department of Theoretical and Applied Mechanics, Cornell University, Ithaca, New York 14853-1503, USA
e-mail: strogatz@cornell.edu
†Department of Engineering, University of Cambridge, Cambridge CB2 1PZ, UK
‡University of Maryland, College Park, Maryland 20742, USA
§Fachbereich Physik, Philipps-Universität Marburg, 35032 Marburg, Germany

1. Dallard, P. et al. Struct. Eng. **79**, 17–33 (2001).
2. Dallard, P. et al. J. Bridge Eng. **6**, 412–417 (2001).
3. McRobie, A., Morgenthal, G., Lasenby, J. & Ringer, M. Proc. Inst. Civ. Eng. Bridge Eng. **156**, 71–79 (2003).
4. Roberts, T. M. Proc. Inst. Civ. Eng. Bridge Eng. **156**, 155-160 (2003).
5. Newland, D. E. Proc. Inst. Mech. Eng. **218**, 477–492 (2004).
6. Nakamura, S. J. Struct. Eng. **130**, 32–37 (2004).
7. Glass, L. & Mackey, M. C. From Clocks to Chaos: The Rhythms of Life (Princeton Univ. Press, Princeton, 1988).
8. Winfree, A. T. The Geometry of Biological Time 2nd edn (Springer, New York, 2001).
9. Kuramoto, Y. Chemical Oscillations, Waves and Turbulence (Springer, Berlin, 1984).
10. Strogatz, S. H. Physica D **143**, 1–20 (2000).

associated liquids (water and alcohols) with time can be attributed to flow-induced solvent ordering or the formation of bubbles (our unpublished results).

We conclude that these high fluid velocities are possible because of a frictionless surface at the carbon-nanotube wall. This result could be explained in conventional terms of slip lengths, which are remarkably long. The slip length is an extrapolation of the extra pore radius required to give zero velocity at a hypothetical pore wall (the boundary condition for conventional materials). The observed slip lengths (3–70 µm) are much longer than the pore radius (3.5 nm) that is consistent with a nearly frictionless interface. The slip length decreases as solvents become more hydrophobic (Table 1), which indicates stronger interaction with the carbon-nanotube wall. The observed flow velocities for water (10–44 cm s^{-1}) are close to the extrapolated rate predicted for water flow through single-walled carbon nanotubes (about 90 cm s^{-1})[4]. Butane flows through carbon nanotubes at about 26 cm s^{-1} (ref. 6), which is consistent with our measurement for hexane.

These results show that the speed of fluid flow through the aligned carbon-nanotube membrane approaches that through biological channels. The membrane fabrication is scalable to large areas, which could be useful industrially for chemical separations; chemical functionality is near the core entrance[9] and each side of the membrane can be independently modified with different functional groups[10]. These advantages also make the aligned carbon-nanotube membrane a promising mimic of protein channels for transdermal drug delivery and selective chemical sensing.

Mainak Majumder*, Nitin Chopra*, Rodney Andrews†, Bruce J. Hinds*
*Chemical and Materials Engineering Department, University of Kentucky, Lexington, Kentucky 40506, USA
e-mail: bjhinds@engr.uky.edu
†Center for Applied Energy Research, Lexington, Kentucky 40511, USA

NANOSCALE HYDRODYNAMICS

Enhanced flow in carbon nanotubes

Nanoscale structures that could mimic the selective transport and extraordinarily fast flow possible in biological cellular channels would have a wide range of potential applications. Here we show that liquid flow through a membrane composed of an array of aligned carbon nanotubes is four to five orders of magnitude faster than would be predicted from conventional fluid-flow theory. This high fluid velocity results from an almost frictionless interface at the carbon-nanotube wall.

Biological channels act as chemically selective gatekeepers and have protein walls that allow extremely rapid transit[1]. Nanometre-scale pores with chemical selectivity have been prepared[2,3] but fluid flow through them is slow: this limitation is predicted by the Hagen–Poiseuille equation and is because conventional laminar flow has zero fluid velocity at the pore walls.

In theory, the flow of molecules inside carbon nanotubes could be much faster. Water should be able to flow fast through hydrophobic single-walled carbon nanotubes because the process creates ordered hydrogen bonds between the water molecules[4]. Ordered hydrogen bonds between water molecules and the weak attraction between the water and smooth carbon-nanotube graphite sheets should then result in almost frictionless and very rapid flow[4]. If a theoretical volume rate comparable to that of the protein channel aquaporin-1 (ref. 4) is divided by the carbon-nanotube cross-sectional area, the expected water flow velocity is about 90 cm s^{-1}. Fast flow velocities are also predicted just from the frictionless nature of the carbon-nanotube walls[5] and from the rapid diffusion of hydrocarbons[6,7].

To realize these high flow velocities, we used a freshly fabricated membrane consisting of aligned multiwalled carbon nanotubes, with graphitic inner cores (diameter about 7 nm) and a high area density (5×10^{10} per cm^2), crossing a solid polystyrene film[8]. We measured the flow of water and a variety of solvents through this membrane at about 1 atm applied pressure (Table 1). In a control experiment, we verified that no macroscopic defects were present in the membrane and determined the available pore area (see supplementary information).

We found that the flow rates are four to five orders of magnitude faster than conventional fluid flow would predict through pores of 7 nm diameter. Contrary to predictions based on hydrodynamics, the flow rate does not decrease with increased viscosity (compare hexane and water in Table 1). The results also indicate that flow velocity, when adjusted for differences in viscosity, increases for more hydrophilic fluids. The flow of hydrogen-bonded fluids decreases after a few minutes, but this does not occur with alkanes or aqueous solutions of potassium chloride. Reduction in the flow of

Table 1 | Pressure-driven flow through aligned MWCNT membrane

Liquid	Initial permeability*	Observed flow velocity†	Expected flow velocity†	Slip length (mm)
Water	0.58	25	0.00057	54
	1.01	43.9	0.00057	68
	0.72	9.5	0.00015	39
Ethanol	0.35	4.5	0.00014	28
iso-Propanol	0.088	1.12	0.00077	13
Hexane	0.44	5.6	0.00052	9.5
Decane	0.053	0.67	0.00017	3.4

MWCNT, multiwalled carbon nanotube. For details of methods, see supplementary information. *Units, cm^3 per cm^2 min bar. †Flow velocities in cm s^{-1} at 1 bar. Expected flow velocity is that predicted from conventional flow.

1. Hille, B. Ionic Channels of Excitable Membranes (Sinauer, Sunderland, Massachusetts, 1984).
2. Jirage, K. B., Hulteen, J. C. & Martin, C. R. Science **278**, 655–658 (1997).
3. Klein, E. J. Membr. Sci. **179**, 1–27 (2000).
4. Hummer, G., Rasaih, J. C. & Noworyta, J. P. Nature **414**, 188–190 (2001).
5. Sokhan, V. P., Nicholson, D. & Quirke, N. J. Chem. Phys. **117**, 8531–8539 (2002).
6. Skoulidas, A. I., Ackerman, D. M., Johnson, J. K. & Sholl, D. S. Phys. Rev. Lett. **89**, 185901 (2002).
7. Mao, Z. & Sinnott, S. B. J. Phys. Chem. B **105**, 6916–6924 (2001).
8. Hinds, B. J. et al. Science **303**, 62–65 (2004).
9. Majumder, M., Chopra, N. & Hinds, B. J. J. Am. Chem. Soc. **127**, 9062–90670 (2005).
10. Chopra, N., Majumder, M. & Hinds, B. J. Adv. Funct. Mater. **15**, 858–864 (2005).

BRIEF COMMUNICATIONS ARISING online
↪ www.nature.com/bca see Nature contents.

COLLOID SCIENCE

Non-spherical bubbles

Surface tension gives gas bubbles their perfect spherical shape by minimizing the surface area for a given volume[1]. Here we show that gas bubbles and liquid drops can exist in stable, non-spherical shapes if the surface is covered, or 'armoured', with a close-packed monolayer of particles. When two spherical armoured bubbles are fused, jamming of the particles on the interface supports the unequal stresses that are necessary to stabilize a non-spherical shape.

We have previously described a microfluidic method for producing spherical armoured bubbles that are all the same size[2]. The rigid particles straddle the gas–liquid interface and have mechanical properties distinct from either constituent, forming what we call an interfacial composite material.

We find that fusion of these armoured bubbles, achieved by squeezing the bubbles between two glass plates, produces a stable ellipsoidal shape (Fig. 1 a–c) (for methods, see supplementary information). The fused armoured bubble is unable to relax to a spherical shape by expelling particles: instead, the jamming[2] of the particles on the closed interface, which is mediated by surface tension, leads to non-minimal shapes.

The non-trivial geometry of these bubbles provides a natural means of understanding the state of stress in the interfacial composite material. A balance of normal stresses at the bubble surface demands that

$$\Delta P = \frac{\sigma_1}{R_1} + \frac{\sigma_2}{R_2}$$

where ΔP is the pressure jump across the surface, R_1 and R_2 are the local principal radii of curvature, and σ_1 and σ_2 are the corresponding principal resultants of surface stress. Therefore, if $R_1 \neq R_2$, as is the case for non-spherical bubbles, then $\sigma_1 \neq \sigma_2$. A simple fluid interface at equilibrium cannot support unequal stresses[3]. But the bubble does, because of steric jamming[4] of the armour particles, so we term the interfacial composite material a solid.

The armoured bubbles can be remodelled into various stable anisotropic shapes because the interfacial composite material is able to undergo extensive particle-scale rearrangements in order to accommodate external inhomogeneous stresses (our manuscript in preparation). These shape changes occur with apparently no hysteresis and at relatively low forces, which is equivalent to perfect plasticity in continuum mechanics.
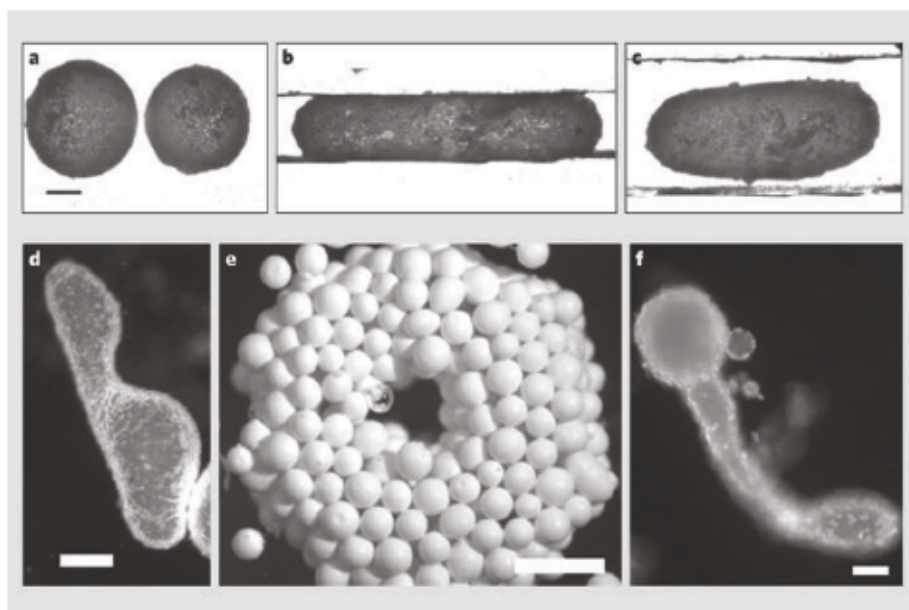
High aspect-ratio shapes with saddle curvature can be maintained on the armoured bubbles (Fig. 1d). This feature may be exploited to change the topology of the bubble by introducing a hole into the object, thereby creating a stable genus-1 toroid (Fig. 1e). The change in topology is irreversible[5], and seems to be the only permanent change associated with the manipulation of the interfacial composite material.

We have found that interfacial jamming is a general phenomenon that occurs with particle types such as polymethylmethacrylate, gold and zirconium oxide, and that spans four orders of magnitude in particle and bubble sizes. Similar effects are evident with liquid droplets of mineral oil that are covered with rigid particles (Fig. 1f).

Stable, non-spherical shapes of pressurized systems that have no obvious source of a stress-bearing network have been reported for dirty air bubbles in the ocean[6] and for various cellular organelles[7]. Also, systems such as gelled lipids on air bubbles[8] and protein-coated vesicles[9] show plasticity. We propose that a generic interfacial jamming transition may explain the mechanical properties and structural stability of these diverse systems.

Anand Bala Subramaniam, Manouk Abkarian,
L. Mahadevan, Howard A. Stone
Division of Engineering and Applied Sciences,
Harvard University, Cambridge, Massachusetts
02138, USA
e-mail: has@deas.harvard.edu

1. Boys, C. V. *Soap Bubbles — Their Colours and the Forces which Mould Them* (Dover, New York, 1959).
2. Bala Subramaniam, A., Abkarian, M. & Stone, H. A. *Nature Mater.* **4**, 553–556 (2005).
3. Vella, D., Aussillous, P. & Mahadevan, L. *Europhys. Lett.* **68**, 212–218 (2004).
4. Liu, A. J. & Nagel, S. R. *Nature* **396**, 21–22 (1998).
5. Alexandrov, P. S. *Elementary Concepts of Topology* (Dover, New York, 1961).
6. Johnson, B. D. & Cooke, R. C. *Science* **213**, 209–211 (1981).
7. Joachim, S., Jokitalo, E., Pypaert, M. & Warren, G. *Nature* **407**, 1022–1026 (2000).
8. Kim, D. H., Costello, M. J., Duncan, P. B. & Needham, D. *Langmuir* **19**, 8455–8466 (2003).
9. Ratanabanangkoon, P., Gropper, M., Merkel, R., Sackmann, E. & Gast, A. P. *Langmuir* **19**, 1054–1062 (2003).

Figure 1 | Non-spherical gas bubbles. In a–d, the bubbles are covered with charge-stabilized, fluorescent polystyrene beads, each of 2.6 μm diameter. **a,** Two initially spherical armoured bubbles. **b,** The bubbles are compressed between two glass plates (see supplementary information for details), which exposes naked interfaces that spontaneously coalesce. **c,** The gas bubble maintains a stable ellipsoidal shape even after the side plates are removed. **d,** Armoured bubble with a stable saddle shape. **e,** The ability to maintain a saddle curvature allows a hole to be introduced into the bubble to create a permanent change of topology into a genus-1 toroid; here the particles are ground zirconium, of average diameter 200 μm. **f,** Non-spherical shapes can be similarly maintained on mineral-oil droplets in water armoured with 4.0-μm fluorescent polystyrene particles. Scale bars (μm): a–c, 100; d, 200; e, 500; and f, 16.

ERRATUM

Nanoscale hydrodynamics: Enhanced flow in carbon nanotubes
Mainak Majumder, Nitin Chopra, Rodney Andrews, Bruce J. Hinds
Nature **438**, 44 (2005)

In Table 1, slip lengths are in micrometres (and not millimetres, as published).
doi:10.1038/438930b